Adaptive Control of Vehicle Steering-by-Wire System with Varying-Degree Lyapunov Function and Deterministic Robust Control Augmentation

Xingyu Zhou, Hyunjin Ahn, Yung-Chi Kung, Heran Shen, and Junmin Wang*, *IEEE Fellow*Walker Department of Mechanical Engineering
University of Texas at Austin

Abstract—Existing adaptive control designs for vehicle steering-by-wire (SbW) systems mainly rely on quadratic Lyapunov functions, providing (global) stability and, at best, (global) asymptotic convergence of certain closed-loop signals. However, these approaches generally lack assurance in transient performance. In this paper, we introduce a novel adaptive control scheme aimed to enhance and guarantee the transient performance of the adaptive SbW control system. This approach integrates a varying-degree Lyapunov function with deterministic robust control. The new adaptive control scheme is derived in a general context, applicable to a class of singleinput, parametrically uncertain, nonlinear dynamic systems in Brunovsky form. We then apply this general theoretical result to develop an adaptive controller for the SbW system. Using a highfidelity moving-base driving simulator, we demonstrate the transient performance improvement of the new adaptive SbW controller compared to a baseline method.

Keywords: transient performance, adaptive control, steering control

I. INTRODUCTION

A. Background

Vehicle steering-by-wire (SbW) technology represents a major innovation within the automotive automation landscape, reshaping traditional steering systems at their core [1]. Through the incorporation of electromechanical sensing and actuation in conjunction with by-wire controls, this technology grants drivers intelligent and customizable steering responses [2]. Besides, the elimination of a physical steering column enhances driving safety by reducing collision-related risks [3]. What makes the SbW technology even more promising is its seamless compatibility with automated/autonomous driving systems, promoting it a well-suited solution for the intricate demands of self-driving functionalities [4],[5]. Recent studies also highlight how SbW systems can enhance shared steering control between humans and automation systems [2],[5],[6]. These promising aspects of SbW technology have spurred a surge in research efforts dedicated to advancing its capabilities, particularly in SbW controls.

B. Literature Overview

A core component of the SbW system is a properly crafted control system. This control system plays a pivotal role in effectively managing the steering servo motor, ensuring it produces the desired steering torque. This, in turn, ensures that the vehicle's front road wheels accurately track the steering wheel's reference command (produced either by the driver and/or the automated driving system). In the literature, a gamut

of control approaches for vehicle SbW systems has been documented. These methods involve robust control techniques, including H_{∞} control [7], sliding-mode control [8], and others. Adaptive control [9] and iterative learning control [10], among others, have also been studied.

Markedly, the adaptive control method has gained considerable interest in formulating the SbW control law. This is primarily due to its capability to address model uncertainties, such as electromechanical parameter perturbations [18], through real-time learning and adaptation [9]. In [10], an adaptive sliding-model control strategy was introduced for SbW system control, with a noteworthy feature being its adaptive compensation for the self-aligning moment. In [11], an SbW control law based on the adaptive backstepping control method was presented. To enhance its robustness, this adaptation mechanism incorporated a novel leakage modification, ensuring the boundedness of adaptive control parameters. In a distinct approach, authors in [12] ingeniously unified adaptive sliding-mode control with an event-triggered mechanism to govern the SbW system. The introduction of the event-triggered scheme yielded benefits in conserving communication resources within the control system. Recent studies explored the fusion of adaptive control and artificial neural networks for SbW system control, demonstrating the neural network's effectiveness in modeling complex uncertainties [13].

C. Research Gap and Our Contribution

While the previous studies have shown effectiveness in controlling the adaptive SbW system and adequately coping with system uncertainties through adaptation, there may still be considerable room for improving the control system's performance. Particularly, the majority of adaptive SbW controllers found in the literature can only theoretically guarantee (global) stability and at best (global) asymptotic convergence of certain closed-loop signals. However, transient behaviors, which are equally, if not more critical than steady-state characteristics, tend to receive less attention. Consequently, these existing adaptive SbW controllers may exhibit inadequate transient performance (e.g., slow convergence, oscillatory responses, significant overshoots, etc.). In response to this research gap, the contribution of this paper is dedicated to enhancing the transient performance from two perspectives. First, virtually all existing adaptive SbW controllers in the literature are established with quadratic Lyapunov functions (QLF). Departing from such a mainstream, we originate a new adaptive control scheme

*Corresponding Author. Xingyu Zhou (e-mail: xingyu.zhou@austin.utexas.edu); Hyunjin Ahn (e-mail: hjahn@utexas.edu); Yung-Chi Kung (e-mail: yung-chi.kung@utexas.edu); Heran Shen (e-mail:

hs29354@utexas.edu); Junmin Wang (e-mail: JWang@austin.utexas.edu). This work was partially supported by NSF Award 2312466.

based on a varying-degree Lyapunov function (VDLF) to tackle the SbW control design problem. VDLF-based adaptive control law, as demonstrated later, outperforms the traditional QLF-based method by offering superior transient and convergence properties. Second, we propose a systematic integration of VDLF-based adaptive control with deterministic robust control (DRC). This integration further bolsters the transient performance of the closed-loop system. Augmenting DRC ascertains exponentially fast transient performance with prescribed precision.

This novel adaptive control scheme is derived for a general class of single-input, parametrically uncertain, nonlinear dynamic systems in Brunovsky form, making it applicable to a range of physical systems. In this paper, the spirit of the proposed solution will be elaborated through its application in the adaptive SbW control law synthesis.

D. Paper Organization

The paper proceeds as follows: In Section II, we establish the theoretical foundation by deriving an adaptive control law (integrating VDLF and DRC) for a general $n^{\rm th}$ -order, single-input, parametrically uncertain, nonlinear dynamic system in Brunovsky form. This section includes analyses of closed-loop stability, signal convergence, and boundedness, along with a theoretical comparison to the conventional QLF-based adaptive control solution. Section III applies the proposed adaptive control scheme to develop an adaptive controller for the SbW system. Section IV presents experimental results comparing the suggested SbW adaptive controller with a baseline QLF-based solution. Section V concludes the paper.

II. THEORETICAL FOUNDATION

This section details the establishment of the adaptive control law, which synergizes the VDLF and the DRC, for an $n^{\rm th}$ -order, single-input, parametrically uncertain, nonlinear dynamic systems in Brunovsky form. We will begin by formulating the control problem, followed by the synthesis of the adaptive control law and subsequent stability analysis. We will then compare certain theoretical properties of the proposed adaptive control law to those of the traditional QLF-based solution.

A. Control Problem Formulation

To demonstrate the essence of the proposed adaptive control design strategy, we will examine a class of single-input uncertain nonlinear dynamic systems that can be transformed into the following form $(x, u \in \mathbb{R})$:

$$x^{(n)} = \sum_{i=1}^{M} a_i f_i(x, \dot{x}, \ddot{x}, \dots x^{(n-1)}, w) + bg(x, \dot{x}, \ddot{x}, \dots x^{(n-1)}, w)u.$$
(1)

In this context, we have $w \in \mathbb{R}^m$ being a measurable exogenous vector. Both $f_i(\bullet, \bullet) \colon \mathbb{R}^n \times \mathbb{R}^m \to \mathbb{R}$ and $g(\bullet, \bullet) \colon \mathbb{R}^n \times \mathbb{R}^m \to \mathbb{R}$ are known Lipschitz functions. Additionally, model parameters $a_i \in \mathbb{R}$ and $b \in \mathbb{R}$ are assumed to be unknown constants or exhibit slow variations. It's important to note that we further assume b, the high-frequency gain, to be non-zero with known sign, along with $g(\bullet, \bullet)$ to be non-zero within the system's operational range,

ensuring controllability. The dynamic system described in (1) serves as a model for a range of physical systems.

To maintain clarity and succinctness in notation, we will henceforth omit the explicit function input arguments for all nonlinear functions (except when it is needed for emphasis). In other words, functions $f_i(\bullet,\bullet)$ and $g(\bullet,\bullet)$, originally defined as functions of x and its derivatives up to the $(n-1)^{\text{th}}$ order and w, will be represented simply as f_i and g in the subsequent discussion. This allows compact expression of the single-input, uncertain, nonlinear system in what is referred to as the controllable canonical form:

$$\frac{d}{dt} \begin{pmatrix} x \\ \dot{x} \\ \vdots \\ x^{(n-1)} \end{pmatrix} = \begin{pmatrix} \dot{x} \\ \ddot{x} \\ \vdots \\ \sum_{i=1}^{M} a_i f_i + b g u \end{pmatrix}.$$
(2)

The primary objective of our control design is to ensure that x closely follows a bounded reference command $x_r \in \mathbb{R}$. We adopt the assumption that x_r is sufficiently smooth, i.e., it possesses at least n-fold differentiability with respect to time. With this in mind, we then introduce reference-tracking errors, denoted as $e^{(k)} \triangleq x^{(k)} - x_r^{(k)}$, $k = 0, \dots, N$. Accordingly, the dynamics associated with these tracking errors can be expressed as follows:

$$\frac{d}{dt} \begin{pmatrix} e \\ \dot{e} \\ \vdots \\ e^{(n-1)} \end{pmatrix} = \begin{pmatrix} \dot{e} \\ \ddot{e} \\ \vdots \\ b \left(gu + \sum_{i=1}^{M} \theta_i f_i - b^{-1} x_r^{(n)} \right) \end{pmatrix}, \quad (3)$$

where $(\theta_1, ..., \theta_M) = (b^{-1}a_1, ..., b^{-1}a_M)$. We assume $\theta_i \in (\underline{\theta_i}, \overline{\theta_i})$ and $\underline{\theta_i}$, $\overline{\theta_i}$ are given *a prior* or can be estimated in practice.

We define the following perturbation variable $Y \in \mathbb{R}$ (a composite error) to facilitate the subsequent control law synthesis:

$$\Upsilon \triangleq \varsigma_{n-1} e^{(n-1)} + \varsigma_{n-2} e^{(n-2)} + \dots + \varsigma_0 e.$$
 (4)

In (4), parameters $\zeta_j \in \mathbb{R}_+$, $j = 0, \dots, n-1$ are judiciously selected to ensure that matrix A_r , defined as follows, is Hurwitz.

$$A_r \triangleq \begin{pmatrix} 0 & I_{n-1} \\ \mathcal{F} \end{pmatrix}, \mathcal{F} \triangleq \begin{pmatrix} -\varsigma_0 & \cdots & -\varsigma_{n-2} & -\varsigma_{n-1} \end{pmatrix}.$$
 (5)

We also enforce $\zeta_{n-1} = 1$.

Accordingly, error dynamics as in (3) can be equivalently transformed into a cascaded system $(k \in \mathbb{R}^+)$:

ed into a cascaded system
$$(k \in \mathbb{R}^+)$$
:
$$\frac{d}{dt} \begin{pmatrix} e \\ \dot{e} \\ \vdots \\ e^{(n-2)} \end{pmatrix} = \begin{pmatrix} \dot{e} \\ \vdots \\ \Upsilon - \sum_{j=0}^{n-2} \zeta_j e^{(j)} \end{pmatrix},$$

$$\dot{\Upsilon} = -k\Upsilon + b \left(gu + \sum_{i=1}^{M+1} \theta_i f_i \right). \tag{6}$$

In (6), $\theta_{M+1} \triangleq b^{-1}$ and $f_{M+1} \triangleq -x_r^{(n)} + k\Upsilon + \sum_{j=0}^{n-2} \varsigma_j e^{(j+1)}$. Supposing θ_i in (5) were known (ideal case), the idealized control law,

$$u = -\frac{1}{g} \sum_{i=1}^{M+1} \theta_i f_i, \tag{7}$$

would render Y's dynamics Hurwitz so that Y will converge to zero exponentially fast. As a result, $(e, ..., e^{(n-1)})$ will converge to zero thanks to the vanishing perturbation Y. Nevertheless, in real-world applications, obtaining sufficiently accurate values for θ_i can be challenging, if not impossible. These values can also exhibit (slow) changes due to variations in operating conditions. A practical approach to tackle this parametric uncertainty is to implement a direct adaptive control scheme that can dynamically compensate for these uncertainties in real-time. This involves substituting θ_i in the nominal control law with their online estimated counterparts, denoted as $\hat{\theta}_i$ (so-called certainty equivalence).

B. VDLF-based and DRC-augmented Adaptive Control

Strategically integrating VDLF and DRC, a robust adaptive control law is formulated as follows:

$$u = u_A + u_D, (8)$$

where u_A and u_D denote the VDLF-based adaptive compensation part and the DRC augmentation, respectively. u_A and u_D are designed as:

$$u_{A} = -\frac{1}{g} \sum_{i=1}^{M+1} \hat{\theta}_{i} f_{i}, \qquad (9)$$

$$u_D = -\frac{\operatorname{sgn}(b)}{g} \sum_{i=1}^{M+1} \mathcal{P}_i \tanh(\epsilon^{-1} \Upsilon \mathcal{P}_i).$$
 (10)

For u_A , a projection-based adaptation law for $\hat{\theta}_i$ is formulated as (we adopt the projection scheme from [14]):

$$\hat{\theta}_{i} = \operatorname{Proj}_{\left[\underline{\theta}_{i}, \overline{\theta}_{i}\right]} \left(\widecheck{\theta}_{i} \right) = \begin{cases} \widecheck{\theta}_{i}, \forall \widecheck{\theta}_{i} \in \left[\underline{\theta}_{i}, \overline{\theta}_{i}\right] \\ \underline{\theta}_{i}, \forall \widecheck{\theta}_{i} \in \left(-\infty, \underline{\theta}_{i}\right). \\ \overline{\theta}_{i}, \forall \widecheck{\theta}_{i} \in \left(\overline{\theta}_{i}, \infty\right) \end{cases}$$
(11)

The rationale behind implementing the projection scheme in this context is based on the assumption that $\theta_i \in (\underline{\theta}_i, \overline{\theta}_i)$ and that $\underline{\theta}_i$ and $\overline{\theta}_i$ are either known beforehand or can be estimated in practical scenarios. With these predefined bounds in place, the projection scheme in (11) offers two advantages: it prevents unnecessary learning efforts beyond the feasible range and enhances the adaptative mechanism's robustness against unmodeled dynamics and disturbances as it guarantees boundedness for $\hat{\theta}_i$. The auxiliary parameter $\check{\theta}_i$ is adapted as,

 $\dot{\theta}_i = \lambda_i \operatorname{sgn}(b) |\Upsilon|^{s(|\Upsilon|)} \operatorname{sgn}(\Upsilon) \mathcal{H} f_i - l_i. \tag{12}$ In (12), $l_i \triangleq \sigma_i (\breve{\theta}_i - \widehat{\theta}_i)$ is a leakage term (to safeguard the boundedness of $\breve{\theta}_i$ in the face of unmodeled dynamics and disturbances), $\lambda_i \in \mathbb{R}^+$ is the rate of adaptation, $\sigma_i \in \mathbb{R}^+$ is the rate of leakage, and

$$\mathcal{H} \triangleq 1 + s(|Y|) + \frac{\partial s(|Y|)}{\partial |Y|} |Y| \ln(|Y|). \tag{13}$$

It is important to note that while $\ln(|Y|)$ becomes unbounded as |Y| approaches zero, the value of \mathcal{H} remains bounded because $\lim_{|Y|\to 0} |Y| \ln(|Y|) = 0$. To prevent numerical overflow in practice, we can substitute $\ln(|Y|)$ with $\ln(|Y| + Y_s)$, where

 $\Upsilon_s \in \mathbb{R}^+$ is chosen sufficiently small.

The degree function s(|Y|) in (13) is designed as:

$$s(|\Upsilon|) \triangleq \alpha_s + \frac{1}{2}(\beta_s - \alpha_s) \{ \tanh[\gamma_s(|\Upsilon| - 1)] + 1 \}. \quad (14)$$

The design parameters for s(|Y|) are specified as follows: $\alpha_s \in (0,1)$, $\beta_s \in (1,\infty)$, and $\gamma_s \in \mathbb{R}^+$. As per the design, s(|Y|) is guaranteed to have a lower bound of α_s and is, therefore, always positive. It is essential to emphasize that when selecting the value of γ_s , it should be sufficiently large to enable rapid switching between α_s and β_s .

Meanwhile, for u_D , we design \mathcal{P}_i as,

$$\mathcal{P}_i \triangleq \sqrt{r_i^2 + \Delta \theta_i^2 f_i^2},\tag{15}$$

where $r_i \in \mathbb{R}$ shall be chosen sufficiently close to zero and $\Delta\theta_i \triangleq \overline{\theta}_i - \underline{\theta}_i$ is the projection interval width for $\hat{\theta}_i$. Moreover, $\epsilon \in \mathbb{R}^+$ inside $\tanh(\bullet)$ in (10) is a design parameter to prescribe the precision of the DRC's guaranteed transient convergence.

C. Closed-loop Stability Analysis

With the definition $\tilde{\theta}_i \triangleq \hat{\theta}_i - \theta_i$ as the control parameter adaptation error, the dynamics for the perturbation Υ , under the effectuation of the robust adaptive control law as in (8) – (10), can be expressed as follows:

$$\dot{\Upsilon} = -k\Upsilon - b \sum_{i=1}^{M+1} \tilde{\theta}_i f_i - |b| \sum_{i=1}^{M+1} \mathcal{P}_i \tanh(\epsilon^{-1} \Upsilon \mathcal{P}_i). \quad (16)$$

Next, two short facts and two lemmas are offered to facilitate the subsequent analysis.

Fact 1. $\mathcal{P}_i \geq |\Delta \theta_i f_i|$. This fact is straightforward to prove as $\mathcal{P}_i \triangleq \sqrt{r_i^2 + \Delta \theta_i^2 f_i^2} \geq \sqrt{\Delta \theta_i^2 f_i^2} = |\Delta \theta_i f_i|$.

Fact 2. $\forall v \in \mathbb{R}, \epsilon \in \mathbb{R}_+, \ 0 \le |v| - v \tanh(\epsilon^{-1}v) \le \varrho \epsilon^{-1}$ where $\varrho \cong 0.279$. This fact can also be easily verified with an elementary calculus analysis.

Lemma 1. [14] The scaler function $V_{\widetilde{\Theta}}$ defined below is positive semidefinite:

$$V_{\widetilde{\Theta}} \triangleq \sum_{i=1}^{M+1} \frac{|b|}{2\lambda_i} \left[\left(\widecheck{\theta}_i - \theta_i \right)^2 - \left(\widecheck{\theta}_i - \widehat{\theta}_i \right)^2 \right]. \tag{17}$$

Lemma 2. With a sufficiently large γ_s , \mathcal{H} as defined in (13) is positive semidefinite and bounded. Lemma 2 can be proved with an elementary calculus analysis.

With the afore-listed facts and lemmas, the main theorem is now presented.

Theorem 1. We denote the error vector as $z = (e, ..., e^{(n-1)})$. For the process dynamics as described in (6), the following results hold if the VDLF and DRC-based robust adaptive control law is applied:

a) The closed-loop adaptive system is stable in the large and $\lim_{t\to\infty} \Upsilon(t), z(t) = 0.$

b)
$$|\Upsilon(t)| \le \sqrt{e^{-2k(t-t_0)}\Omega + \frac{\varrho|b|(M+1)}{k\epsilon}}, \forall t \ge t_0 \text{ where } \Omega \triangleq |\Upsilon(t_0)|^2 - \frac{\varrho|b|(M+1)}{k\epsilon}.$$

Proof

To prove Result a), a VDLF (the degree of $|\Upsilon|$ is varying) is conceived as follows:

$$V_1 \triangleq |\Upsilon|^{1+s(|\Upsilon|)} + V_{\widetilde{\Theta}}.\tag{18}$$

It is clear that $V_1 \ge 0$ (as previously established in Lemma 1, $V_{\widetilde{\Theta}} \geq 0$). The degree of $|\Upsilon|$ varies according to the magnitude of $|\Upsilon|$. This marks a notable departure from the conventional QLF-based adaptive control approach, where this exponent remains constant.

Applying the chain rule, we take the time derivative of V_1 , resulting in,

$$\dot{V}_1 = \mathcal{H}[\Upsilon]^{s(|\Upsilon|)} \operatorname{sgn}(\Upsilon) \dot{\Upsilon} + \dot{V}_{\tilde{\Theta}}. \tag{19}$$

Invoking (16) and (17),

$$\dot{V}_{2} = -\mathcal{H}|\mathbf{Y}|^{1+s(|\mathbf{Y}|)} - \mathcal{H}|\mathbf{Y}|^{s(|\mathbf{Y}|)}\operatorname{sgn}(\mathbf{Y})b \sum_{i=1}^{M+1} \tilde{\theta}_{i}f_{i}$$

$$-\mathcal{H}|\mathbf{Y}|^{s(|\mathbf{Y}|)}\operatorname{sgn}(\mathbf{Y})|b| \sum_{i=1}^{M+1} \mathcal{P}_{i} \tanh(\epsilon^{-1}\mathbf{Y}\mathcal{P}_{i})$$

$$+ \sum_{i=1}^{M+1} \frac{|b|}{\lambda_{i}} \left[\tilde{\theta}_{i}\dot{\bar{\theta}}_{i} - (\tilde{\theta}_{i} - \hat{\theta}_{i})\dot{\bar{\theta}}_{i}\right]. \tag{20}$$

Employing the adaptation law of $\dot{\theta}_i$ as stated in (12), \dot{V}_1 can be reduced to,

$$\dot{V}_{1} = -k\mathcal{H}|Y|^{1+s(|Y|)}$$

$$-\mathcal{H}|b| \sum_{i=1}^{M+1} |Y|^{s(|Y|)} \operatorname{sgn}(Y) \mathcal{P}_{i} \tanh(\epsilon^{-1}Y \mathcal{P}_{i})$$

$$+ \sum_{i} \frac{|K_{h}|}{\gamma_{i}} \left[-\sigma_{i} \tilde{\theta}_{i} (\check{\theta}_{i} - \hat{\theta}_{i}) - (\check{\theta}_{i} - \hat{\theta}_{i}) \dot{\hat{\theta}}_{i} \right]. \tag{21}$$

It is easy to verify that $|\Upsilon|^{s(|\Upsilon|)} \operatorname{sgn}(\Upsilon) \sum_{i=1}^{M+1} \mathcal{P}_i \tanh(\epsilon^{-1} \Upsilon \mathcal{P}_i) \ge 0$ term both $|\Upsilon|^{s(|\Upsilon|)} \operatorname{sgn}(\Upsilon) \mathcal{P}_i$ and $\tanh(\varepsilon^{-1} \Upsilon \mathcal{P}_i)$ are odd functions with respect to Y, thereby leading to:

$$\dot{V}_{1} \leq -k\mathcal{H}|Y|^{1+s(|Y|)} + \sum_{i} \frac{|K_{h}|}{\gamma_{i}} \left[-\sigma_{i}\tilde{\theta}_{i}(\check{\theta}_{i} - \hat{\theta}_{i}) - (\check{\theta}_{i} - \hat{\theta}_{i})\dot{\hat{\theta}}_{i} \right]. \tag{22}$$

Now, if $\check{\theta}_i \in (\underline{\theta}_i, \overline{\theta}_i)$, we can conclude $\check{\theta}_i - \hat{\theta}_i = 0$ from the definition of the projection operator. This infers $\dot{V}_1 \leq$ $-k\mathcal{H}|\Upsilon|^{1+s(|\Upsilon|)} \leq 0$. If $\check{\theta}_i \in (-\infty, \theta_i)$, we again observe from the construction of the projection operator that $\hat{\theta}_i = 0$ and $\hat{\theta}_i = \underline{\theta}_i$, along with $\tilde{\theta}_i \leq 0$ and $\breve{\theta}_i - \hat{\theta}_i \leq 0$. Consequently, we can deduce that $\dot{V}_1 \le -k\mathcal{H}|\Upsilon|^{1+s(|\Upsilon|)} \le 0$. Similarly, when $\check{\theta}_i \in (\overline{\theta}_i, \infty)$, we can derive that $\hat{\theta}_i = 0$ and $\hat{\theta}_i = \theta_i$, along with $\tilde{\theta}_i \geq 0$ and $\breve{\theta}_i - \hat{\theta}_i \geq 0$. This, in turn, leads to the same conclusion that $\dot{V}_1 \le -k\mathcal{H}|\Upsilon|^{1+s(|\Upsilon|)} \le 0$.

In summary, the assertion of $\dot{V}_1 \leq -k\mathcal{H}|\Upsilon|^{1+s(|\Upsilon|)} \leq 0$ holds true regardless of the values of $\check{\theta}_i$. This establishes the global stability and signal boundedness of the closed-loop adaptive system.

Furthermore, it is not hard to demonstrate that \ddot{V}_1 remains bounded, indicating the uniform continuity of \dot{V}_1 . Consequently, we can assert that V_1 is bounded from below, as well as \dot{V}_1 is negative semidefinite and uniformly continuous. This leads to the conclusion that $\lim_{t\to\infty} \dot{V}_1(t)=0$ and $\lim \Upsilon(t) = 0$, as substantiated by the Lyapunov-like Lemma presented in [15]. As a result, $(e, ..., e^{(n-2)})$ will converge to zero thanks to the $\lim_{t\to\infty} \Upsilon(t) = 0$ (the subsystem in (6) that admits Υ as an input is Hurwitz). Since Υ is a linear combination of $(e, ..., e^{(n-1)})$, we can conclude that $e^{(n-1)}$ will also converge to zero, meaning $\lim_{t\to\infty} z(t) = 0$. This proves the Result a) of the theorem.

To prove Result b), a different Lyapunov function is devised as follows:

$$V_2 \triangleq \Upsilon^2. \tag{23}$$

as follows:
$$V_2 \triangleq \Upsilon^2. \tag{23}$$
 First, invoking Fact 1, we can assert that:
$$b \sum_{i=1}^{M+1} \tilde{\theta}_i f_i \leq |b| \sum_{i=1}^{M+1} |\Delta \theta_i f_i| \leq |b| \sum_{i=1}^{M+1} \mathcal{P}_i. \tag{24}$$
 With this, the time derivative of V_2 can be carried out as,
$$\dot{V}_2 = -2k\Upsilon^2$$

$$\dot{V}_{2} = -2k\Upsilon^{2}$$

$$-2b\sum_{i=1}^{M+1}\Upsilon\tilde{\theta}_{i}f_{i} - 2|b|\sum_{i=1}^{M+1}\Upsilon\mathcal{P}_{i}\tanh(\epsilon^{-1}\Upsilon\mathcal{P}_{i})$$

$$\leq -2k\Upsilon^{2} + 2|b|\sum_{i=1}^{M+1}[|\Upsilon\mathcal{P}_{i}| - \Upsilon\mathcal{P}_{i}\tanh(\epsilon^{-1}\Upsilon\mathcal{P}_{i})]. \quad (25)$$

At this point, we can apply Fact 2 and establish:

$$\dot{V}_2 \le -2k\Upsilon^2 + 2|b|(M+1)\varrho\epsilon^{-1}.$$
 (26)

By the Comparison Lemma [16], we have $\forall t \geq t_0$,

$$V_{2}(t) \leq e^{-2k(t-t_{0})} \left[V_{2}(t_{0}) - \frac{\varrho|b|(M+1)}{k\epsilon} \right] + \frac{\varrho|b|(M+1)}{k\epsilon}.$$
 (27)

Since $V_2 \triangleq \Upsilon^2$, we can conclude Result b) of the theorem from (27), thus concluding the proof for Theorem 1. \blacksquare

D. Comparison To OLF-based Solution

If we were to design a QLF-based adaptive controller, the updating law for θ_i would be modified as follows (note the difference compared to the VDLF-based updating law in (12):

$$\dot{\theta}_i = \lambda_i \operatorname{sgn}(b) \Upsilon f_i - l_i. \tag{28}$$

 $\dot{\theta}_i = \lambda_i \operatorname{sgn}(b) \Upsilon f_i - l_i. \tag{28}$ At this point, we can discern the fundamental difference between the updating laws in VDLF and QLF approaches. Specifically, the VDLF approach accelerates the trackingerror energy dissipation as the \dot{V}_1 is dynamically scaled with respect to $|\Upsilon|^{1+s(|\Upsilon|)}$. When $|\Upsilon| > 1$, the varying-degree function s(|Y|) switches to $\beta_s \in (1, \infty)$, ensuring $|Y|^{1+s(|Y|)} \ge |Y|^2$. On the other hand, when |Y| < 1, s(|Y|)will switch to $\alpha_s \in (0,1)$, again ensuring $|\Upsilon|^{1+s(|\Upsilon|)} \ge |\Upsilon|^2$. As the experimental results will illustrate, this dynamic energy-dissipation acceleration mechanism introduced by the VDLF-based design fosters an improved transient performance when contrasted with the QLF approach.

Next, Result b) of Theorem I does not typically hold for conventional adaptive control schemes. In other words, conventional schemes do not inherently provide assured exponentially fast transient performance with predefined precision. However, through systematic augmentation of the DRC term u_D , we can ensure that the norm of the perturbation term $\Upsilon(t)$ converges exponentially fast to a prescribed residual set. The size of this residual set can be specified by adjusting the design parameters k or ϵ .

Remark 1: The original proposition for DRC augmentation can be traced back to [15], where it complements a QLF-based adaptive controller. This work extends such a design scheme to a VDLF-based adaptive design.

Remark 2: While drawing inspiration from the nonquadratic Lyapunov function design in [16] and [17], the energy-dissipation acceleration of these works is indeed local. In contrast, the proposed approach in this work achieves a global scale of energy dissipation, which is facilitated by VDLF's smooth switching mechanism.

III. APPLICATION TO SBW SYSTEM CONTROL

According to [8], based on a simplified single-track vehicle model, we shall express the process dynamic model of the SbW system as:

 $J_s\ddot{\delta}_f + B_s\dot{\delta}_f = \kappa_m u - \varepsilon_f \mathrm{sgn}(\dot{\delta}_f) - \tau_{sa},$ (29) where δ_f symbolizes the front road-wheel angle. J_s and B_s are the rotational inertia and the (viscous) frictional coefficient of the steering system, respectively; u denotes the voltage command sent to the steering motor; ε_f is the magnitude of the Coulomb frictional torque; κ_m is the motor constant as $\kappa_m = \kappa_1 \kappa_2 \kappa_3 \kappa_4$ where κ_1 represents the scaling factor converting the steering motor input voltage into the steering motor output torque, κ_2 denotes the gear ratio of the gear head, κ_3 signifies the gear ratio of the rack and pinion rack system, and lastly κ_4 serves as the scaling factor that maps the linear motion of the rack to the front road-wheel angle; τ_{sa} , the self-aligning torque, can be approximated as [7, 19-21]:

$$\tau_{sa} = C_f (l_m + l_p) \left(\delta_f - \beta - l_f \frac{\omega_z}{v_r} \right), \tag{30}$$

where C_f is the cornering stiffness of the front axle, l_m and l_p represent the mechanical trail and the pneumatic trail, respectively, β stands for the vehicle sideslip angle, l_f is the vehicle's front wheelbase, ω_z denotes the vehicle yaw rate, and v_x symbolizes the vehicle's longitudinal velocity. The control design objective is to ensure that δ_f accurately follows a bounded and smooth reference command, δ_r , which can originate from either the human driver or the automated driving system. This control objective shall remain robust even in the presence of potential uncertainties in the aforementioned SbW model parameters.

Following the derivation in Sec. II, a control-oriented SbW model can be established as $(\delta_e \triangleq \delta_f - \delta_r, \Upsilon = \varsigma_0 \delta_e + \dot{\delta}_e)$:

$$\frac{d}{dt}e = \Upsilon - \varsigma_0 \delta_e,$$

$$\dot{\Upsilon} = -k\Upsilon + b\left(u + \sum_{i=1}^5 \theta_i f_i\right),$$
(31)

where $b = \kappa_m J_s^{-1}$, $\theta_1 = B_s \kappa_m^{-1}$, $\theta_2 = \varepsilon_f \kappa_m^{-1}$, $\theta_3 = C_f (l_m + l_p) \kappa_m^{-1}$, $\theta_4 = C_f (l_m + l_p) l_f \kappa_m^{-1}$, $\theta_5 = b^{-1}$ and $f_1 = -\dot{\delta}_f$, $f_2 = -\mathrm{sgn}(\dot{\delta}_f)$, $f_3 = \beta - \delta_f$, $f_4 = \frac{\omega_z}{v_x}$, $f_5 = -\ddot{\delta}_r + k\Upsilon + \zeta_0 \dot{\delta}_e$.

With the SbW control-oriented model derived in (31), which aligns with the standard form shown in (6), we can readily apply the general control design framework introduced beyond (8) in Section II to formulate the robust

adaptive SbW controller. According to Theorem 1, the proposed control design can theoretically ascertain that the closed-loop adaptive system is stable in the large and $\lim_{t\to\infty} \Upsilon(t)$, $\delta_e(t)$, $\delta_e(t)=0$. Further, the DRC augmentation further ensures the prescribed exponential convergence of the norm of the perturbation variable Υ .

IV. EXPERIMENTAL VALIDATION

A. Experiment Setup

For the experimental verification of the adaptive controller's effectiveness, we employ a high-fidelity driving simulation setup [22] as Figure 1 shows. As depicted on the left, the moving-base driving simulator system incorporates a physical SbW system, a six-degree-of-freedom Steward motion platform, and a cylindrical projection screen. Furthermore, depicted on the right, a dSPACE SCALEXIO hardware-inthe-loop (HIL) computer is employed to simulate vehicle dynamics (with the software named ASM). The adaptive controller is also programmed within this HIL computer. Communication between the HIL computer and the driving simulator is achieved via CAN Bus and Ethernet. To mimic the vehicle following a slalom path, the reference steering command is designed as $\delta_r = k_r \sin(\varpi_r t)$.

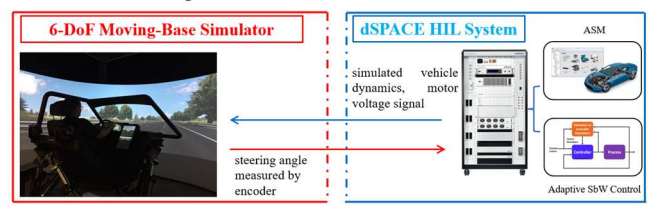


Figure 1. Experimental system setup.

The baseline controller and the proposed controller both utilize the projection operator as described in (11) (with identical projection bounds). The adaptation law for the baseline controller follows the QLF approach outlined in (29). Additionally, the proposed controller incorporates the DRC u_D , a feature absent in the baseline controller.

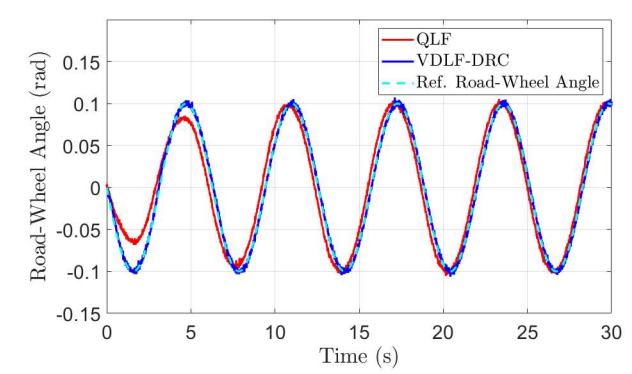


Figure 2. Road-wheel angle responses.

B. Experimental Result

Figure 2 displays the road-wheel angle tracking results for both the proposed robust adaptive control law and the baseline solution. While both approaches demonstrate adequate tracking performance, Figure 3 reveals a substantial advantage of the DRC-augmented VDLF-based design in terms of transient performance. Specifically, the synergy between the VDLF and the DRC leads to rapid convergence of the tracking error towards zero, with a peak error not exceeding 0.01 rad. In contrast, the QLF-based approach exhibits continuous oscillations and slower error decay, even after a 30-second interval, with a significantly larger peak error. The root mean square tracking error with the QLF method is 0.0142 rad, whereas it is reduced to 0.0024 rad (an improvement of over 80%) with the proposed solution.

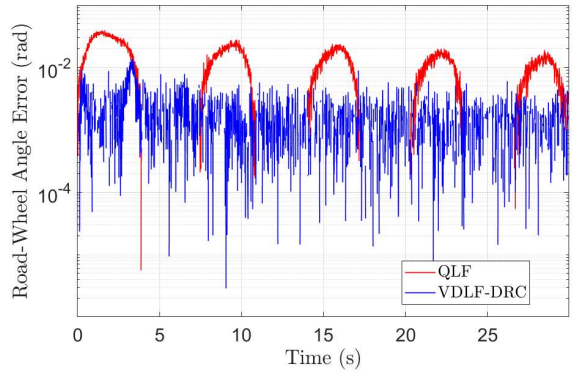


Figure 3. Road-wheel angle tracking errors (semi-log plot).

V. CONCLUSIONS

This paper provides an assured transient performance to the adaptive SbW control system. To achieve this, we propose a novel adaptive control approach that integrates a varyingdegree Lyapunov function with deterministic robust control. This new adaptive control scheme is developed in a general context, making it applicable to a class of single-input, parametrically uncertain, nonlinear dynamic systems in Brunovsky form. We utilize this general theoretical result to design an adaptive controller tailored to the SbW system. Employing a high-fidelity motion-based driving simulator with a physical SbW system, we showcase the enhanced transient performance achieved by the new adaptive SbW controller when compared to a baseline solution. Future research endeavors will prioritize generalizing the proposed adaptive control method to encompass a broader range of nonlinear systems. Further, extensive experimental validation in actual autonomous vehicles will be carried out.

REFERENCES

- [1] M. Bertoluzzo, G. Buja, and R. Menis, "Control schemes for steer-bywire systems," *IEEE Ind. Electron. Mag.*, vol. 1, no. 1, pp. 20–27, 2007, doi: 10.1109/MIE.2007.357171.
- [2] C. Huang, L. Li, Y. Liu, and L. Xiao, "Robust Observer Based Intermittent Forces Estimation for Driver Intervention Identification," *IEEE Trans. Veh. Technol.*, vol. 69, no. 4, pp. 3628–3640, Apr. 2020, doi: 10.1109/TVT.2020.2975366.
- [3] H. Zhang and J. Wang, "Vehicle Lateral Dynamics Control Through AFS/DYC and Robust Gain-Scheduling Approach," *IEEE Transactions on Vehicular Technology*, Vol. 65, No. 1, pp. 489 – 494, 2016, doi: 10.1109/TVT.2015.2391184.
- [4] S. A. Mortazavizadeh, A. Ghaderi, M. Ebrahimi, and M. Hajian, "Recent Developments in the Vehicle Steer-by-Wire System," *IEEE Trans. Transp. Electrific.*, vol. 6, no. 3, pp. 1226–1235, Sep. 2020, doi: 10.1109/TTE.2020.3004694.
- [5] X. Zhou, Z. Wang, H. Shen, and J. Wang, "A Mixed L₁/H₂ Robust Observer With An Application To Driver Steering Torque Estimation for Autopilot-Human Shared Steering," J. Dyn. Sys., Meas., Control, vol. 144, no. 7, p. 071007, Jul. 2022, doi: 10.1115/1.4054262.

- [6] X. Zhou, Z. Wang, and J. Wang, "Driver Steering Torque Estimation via Robust Generalized H₂ Filtering for Human-Automation Shared Driving," *IFAC-PapersOnLine*, vol. 54, no. 20, pp. 895–900, 2021, doi: 10.1016/j.ifacol.2021.11.285.
- [7] Z. Li, X. Jiao, and T. Zhang, "Robust H_∞ Output Feedback Trajectory Tracking Control for Steer-by-Wire Four-Wheel Independent Actuated Electric Vehicles," WEVJ, vol. 14, no. 6, p. 147, Jun. 2023, doi: 10.3390/wevj14060147.
- [8] H. Wang, H. Kong, Z. Man, D. M. Tuan, Z. Cao, and W. Shen, "Sliding Mode Control for Steer-by-Wire Systems With AC Motors in Road Vehicles," *IEEE Trans. Ind. Electron.*, vol. 61, no. 3, pp. 1596–1611, Mar. 2014, doi: 10.1109/TIE.2013.2258296.
- [9] Z. Sun, J. Zheng, Z. Man, and H. Wang, "Robust Control of a Vehicle Steer-by-Wire System Using Adaptive Sliding Mode," *IEEE Trans. Ind. Electron.*, pp. 1–1, 2015, doi: 10.1109/TIE.2015.2499246.
- [10] Z. Sun, J. Zheng, Z. Man, and J. Jin, "Discrete-time iterative learning control for vehicle Steer-by-Wire systems," in 2014 9th IEEE Conference on Industrial Electronics and Applications, 2014, pp. 462– 467. doi: 10.1109/ICIEA.2014.6931208.
- [11] J. Wu, J. Zhang, B. Nie, Y. Liu, and X. He, "Adaptive Control of PMSM Servo System for Steering-by-Wire System With Disturbances Observation," *IEEE Trans. Transp. Electrific.*, vol. 8, no. 2, pp. 2015–2028, Jun. 2022, doi: 10.1109/TTE.2021.3128429.
- [12] H. Li, M. Tie, and Y. Wang, "Event-Triggered Sliding Mode Control Using the Interval Type-2 Fuzzy Logic for Steer-by-Wire Systems with Actuator Fault," *Int. J. Fuzzy Syst.*, vol. 24, no. 7, pp. 3104–3117, Oct. 2022, doi: 10.1007/s40815-022-01323-x.
- [13] Y. Wang, Y. Liu, and Y. Wang, "Adaptive discrete-time NN controller design for automobile steer-by-wire systems with angular velocity observer," *Proc. Inst. Mech. Eng. D: J. Automob. Eng.*, vol. 237, no. 4, pp. 722–736, Mar. 2023, doi: 10.1177/09544070221083426.
- [14] M. R. Akella and K. Subbarao, "A novel parameter projection mechanism for smooth and stable adaptive control," Systems & Control Letters, 54(1), pp. 43–51, 2005, doi: 10.1016/j.sysconle.2004.06.004.
- [15] B. Yao and M. Tomizuka, "Adaptive robust control of SISO nonlinear systems in a semi-strict feedback form," *Automatica*, vol. 33, no. 5, pp. 893–900, May 1997, doi: 10.1016/S0005-1098(96)00222-1.
- [16] X. Zhou, Z. Wang, and J. Wang, "Automated Vehicle Path Following: A Non-Quadratic-Lyapunov-Function-Based Model Reference Adaptive Control Approach With C[∞]-Smooth Projection Modification," *IEEE Trans. Intell. Transport. Syst.*, vol. 23, no. 11, pp. 21653–21664, Nov. 2022, doi: 10.1109/TITS.2022.3182928.
- [17] X. Zhou, Z. Wang, H. Shen, and J. Wang, "A Biquadratic-Lyapunov-Function-based Adaptive Control Methodology with Application to Automated Ground Vehicle Path Tracking," in 2022 American Control Conference (ACC), Atlanta, GA, USA: IEEE, Jun. 2022, pp. 1703–1708. doi: 10.23919/ACC53348.2022.9867878.
- [18] X. Huang and J. Wang, "Real-Time Estimation of Center of Gravity Position for Lightweight Vehicles Using Combined AKF-EKF Method," *IEEE Trans. on Veh. Technol.*, Vol. 63, No. 9, pp. 4221 – 4231, 2014, doi: 10.1109/TVT.2014.2312195.
- [19] J. Wang and R. G. Longoria, "Coordinated and Reconfigurable Vehicle Dynamics Control," *IEEE Transactions on Control Systems Technology*, Vol. 17, No. 3, pp. 723 – 732, 2009, doi: 10.1109/TCST.2008.2002264.
- [20] R. Wang, H. Zhang, and J. Wang, "Linear Parameter-Varying Controller Design for Four-Wheel Independently Actuated Electric Ground Vehicles With Active Steering Systems," *IEEE Trans. Contr. Syst. Technol.*, 22 (4): 1281–1296, 2014, doi: 10.1109/TCST.2013.2278237..
- [21] Y. Chen, C. Hu, and J. Wang, "Motion Planning with Velocity Prediction and Composite Nonlinear Feedback Tracking Control for Lane-Change Strategy of Autonomous Vehicles," *IEEE Transactions* on *Intelligent Vehicles*, 5(1), pp. 63 – 74, 2020, doi: 10.1109/TIV.2019.2955366.
- [22] X. Zhou, and etc., "A Novel Instrumental System for Immersive Simulation-based Driver-in-the-Loop Vehicular Technology Research and Validation," Proceedings of the 2023 IEEE International Automated Vehicle Validation Conference, 2023, doi: 10.1109/IAVVC57316.2023.10328070.